PLOS PATHOGENS

RESEARCH ARTICLE

Kingella kingae PilC1 and PilC2 are adhesive multifunctional proteins that promote bacterial adherence, twitching motility, DNA transformation, and pilus biogenesis

Alexandra L. Sacharok[1‡], Eric A. Porsch[2‡], Taylor A. Yount[1], Orlaith Keenan[1], Joseph W. St. Geme, III[1,2]*

1 University of Pennsylvania Perelman School of Medicine, Philadelphia, Pennsylvania, United States of America, **2** Department of Pediatrics, Children's Hospital of Philadelphia, Philadelphia, Pennsylvania, United States of America

‡ These authors are co-first authors on this work.
* stgemeiiij@chop.edu

Citation: Sacharok AL, Porsch EA, Yount TA, Keenan O, St. Geme JW, III (2022) *Kingella kingae* PilC1 and PilC2 are adhesive multifunctional proteins that promote bacterial adherence, twitching motility, DNA transformation, and pilus biogenesis. PLoS Pathog 18(3): e1010440. https://doi.org/10.1371/journal.ppat.1010440

Editor: Karla J.F. Satchell, Northwestern University Feinberg School of Medicine, UNITED STATES

Received: October 22, 2021

Accepted: March 13, 2022

Published: March 30, 2022

Data Availability Statement: All relevant data are within the manuscript and its Supporting Information files.

Funding: This work was supported by the National Institute of Allergy and Infectious Diseases (https://www.niaid.nih.gov) under award 1R01AI121015 to J.W.S. The funders had no role in study design, data collection and analysis, decision to publish, or preparation of the manuscript.

Abstract

The gram-negative bacterium *Kingella kingae* is a leading cause of osteoarticular infections in young children and initiates infection by colonizing the oropharynx. Adherence to respiratory epithelial cells represents an initial step in the process of *K. kingae* colonization and is mediated in part by type IV pili. In previous work, we observed that elimination of the *K. kingae* PilC1 and PilC2 pilus-associated proteins resulted in non-piliated organisms that were non-adherent, suggesting that PilC1 and PilC2 have a role in pilus biogenesis. To further define the functions of PilC1 and PilC2, in this study we eliminated the PilT retraction ATPase in the Δ*pilC1*Δ*pilC2* mutant, thereby blocking pilus retraction and restoring piliation. The resulting strain was non-adherent in assays with cultured epithelial cells, supporting the possibility that PilC1 and PilC2 have adhesive activity. Consistent with this conclusion, purified PilC1 and PilC2 were capable of saturable binding to epithelial cells. Additional analysis revealed that PilC1 but not PilC2 also mediated adherence to selected extracellular matrix proteins, underscoring the differential binding specificity of these adhesins. Examination of deletion constructs and purified PilC1 and PilC2 fragments localized adhesive activity to the N-terminal region of both PilC1 and PilC2. The deletion constructs also localized the twitching motility property to the N-terminal region of these proteins. In contrast, the deletion constructs established that the pilus biogenesis function of PilC1 and PilC2 resides in the C-terminal region of these proteins. Taken together, these results provide definitive evidence that PilC1 and PilC2 are adhesins and localize adhesive activity and twitching motility to the N-terminal domain and biogenesis to the C-terminal domain.

Competing interests: The authors have declared that no competing interests exist.

Author summary

Kingella kingae is an emerging pediatric pathogen that is a leading cause of osteoarticular infections in children under the age of four. Adherence to epithelial cells is thought to be the first step in *K. kingae* colonization of the host and a prerequisite for invasive disease. Previous work has established that type IV pili are responsible for *K. kingae* adherence to host cells. In this work we identify the *K. kingae* pilus adhesins and localize the adhesive region to the N-terminal domain of these two proteins. We further establish that the two adhesins have distinct binding specificities and also influence other biologic processes. Our study provides new insights into the adherence mechanisms of an increasingly recognized pediatric pathogen and furthers our understanding of *K. kingae* interactions with host cells, identifying new potential therapeutic targets.

Introduction

Kingella kingae is a gram-negative bacterium that colonizes the upper respiratory tract in young children [1]. *K. kingae* colonization is a common occurrence, with approximately 70% of children being colonized by 48 months of age and approximately 10% of young children carrying this bacterium in the oropharynx at any given time [2,3]. While *K. kingae* is usually a commensal organism, on occasion it breaches the epithelial barrier, enters the bloodstream, and spreads hematogenously to sites of infection, causing invasive diseases such as septic arthritis and osteomyelitis [4]. Recent advances in molecular diagnostics have identified *K. kingae* as a leading cause of osteoarticular infections in children between 6 months and 4 years of age [5,6].

Adherence to epithelial cells is believed to be the first step in *K. kingae* colonization of the oropharynx and a prerequisite for invasive disease. *K. kingae* adherence to host cells is a two-step process. The initial step is mediated by type IV pili (T4P), which then retract, bringing the bacterium closer to epithelial cells [7,8]. Retraction displaces the polysaccharide capsule, allowing a surface expressed adhesin called the *Kingella* NhhA homolog (Knh) to mediate the second step required for full-level adherence [8,9]. Strains that lack retractile T4P exhibit an intermediate level of adherence, due to the lack of Knh-mediated adherence [8].

The *K. kingae* PilC1 and PilC2 pilus-associated proteins promote piliation and T4P adhesive activity, with expression of at least one of these proteins being required for piliation and adherence to epithelial cells *in vitro* [7]. These proteins have homologs in other bacterial species, including PilY1 in *Pseudomonas aeruginosa*, PilY1 in *Legionella pneumophila*, and PilC1 and PilC2 in *Neisseria gonorrhoeae* and *Neisseria meningitidis* (constituting the "PilC family"). These PilC family proteins have been shown to play a role in pilus assembly, pilus-mediated adherence, and pilus-mediated twitching motility [10–14]. Previous observations by Morand *et al*. showed that the N-terminal portion of the *N. meningitidis* PilC1 protein was required for PilC1-mediated bacterial adherence in engineered *N. meningitidis* strains [15]. Additionally, in studies of the *N. gonorrhoeae* PilC1 protein, Cheng and colleagues found that full-length recombinant PilC1 was able to block *N. gonorrhoeae* adherence to cultured epithelial cells, while the truncated PilC1 C-terminal domain had no blocking activity [16]. Because *K. kingae* PilC1 and PilC2 are required for surface piliation, it is unclear whether these proteins possess inherent adhesive activity.

The *K. kingae* PilC1 and PilC2 proteins share limited homology with each other, with only 7% identity and 16% similarity overall [7], contrasting with the other known PilC-containing systems, which possess only one protein as in *P. aeruginosa* and *L. pneumophila* or two highly

homologous proteins as in *N. gonorrhoeae* and *N. meningitidis*. Interestingly, in previous work we found that while both *K. kingae* PilC1 and PilC2 were able to promote twitching motility, *K. kingae* exhibited significantly different levels of twitching motility depending on which PilC protein was present, with PilC1 promoting a hyper-motile phenotype in the absence of PilC2 and with PilC2 mediating slightly reduced twitching in the absence of PilC1 [17].

In the present study we examined the specific functions of the *K. kingae* PilC1 and PilC2 proteins. We demonstrate that PilC1 and PilC2 are adhesins and have distinct binding specificities. In addition, we establish that the N-terminal domains of these proteins harbor adhesive activity and are essential for twitching motility. In contrast, the pilus assembly function resides in the C-terminal domain of these proteins.

Results

Elimination of the *K. kingae* PilT retraction ATPase restores surface piliation but not adherence in a Δ*pilC1*Δ*pilC2* mutant

In previous work, we observed that insertional inactivation of *pilC1* and *pilC2* in *K. kingae* resulted in an extreme piliation defect and a non-adherent phenotype [7], suggesting that PilC1 and PilC2 are critical for pilus assembly. To determine whether elimination of PilC1 and PilC2 results in a loss of adhesive activity simply because the resulting organisms are non-piliated, we insertionally inactivated the *K. kingae pilT* gene in the KK03Δ*pilC1*Δ*pilC2* double knockout strain (Table 1), using strains KK03 (wild type), KK03Δ*pilA1* (lacking the major pilin subunit and thus lacking surface fibers), KK03Δ*pilT* (lacking PilT-mediated retraction), KK03Δ*pilC1*Δ*pilT* (lacking PilC1 and PilT-mediated retraction), and KK03Δ*pilC2*Δ*pilT* (lacking PilC2 and PilT-mediated retraction) as controls. As expected, the resulting mutant regained piliation to greater than 90% of the level of wild type strain KK03 as assessed by densitometry analysis of the PilA1 band in pilus preparations normalized to the GAPDH loading control (Fig 1A), consistent with previous work indicating that the *pilT* gene encodes an inner membrane ATPase that mediates pilus retraction in *K. kingae* and *N. gonorrhoeae* [8,18]. As shown in Fig 1B, while strains KK03Δ*pilC1*Δ*pilT* and KK03Δ*pilC2*Δ*pilT* were adherent in assays with Chang cells of HeLa origin, the KK03Δ*pilC1*Δ*pilC2*Δ*pilT* mutant was non-adherent (Fig 1B), supporting the possibility that PilC1 and PilC2 have inherent adhesive activity.

K. kingae PilC1 and PilC2 proteins are adhesins with distinct protein structures

To further explore the possibility that PilC1 and PilC2 are adhesins, we purified recombinant N-terminal 6X histidine-tagged PilC1 and PilC2 (Fig 2A) and examined binding to epithelial cell monolayers. As shown in Fig 2B and 2C, PilC1 exhibited saturable binding with a K_d of 74.4 nM, while PilC2 displayed saturable binding with a K_d of 165.6 nM. Examination of the purified proteins by circular dichroism (CD) spectroscopy revealed that PilC1 and PilC2 have distinct CD spectra when comparing mean residue ellipticity (Fig 2D). Based on the CD spectra, PilC1 is predicted to contain 9.8% helices, 8.3% antiparallel sheets, 21.6% parallel sheets, and 10.9% turns (Fig 2E), while PilC2 is predicted to contain 7.0% helices, 11.6% turns, 42.5% antiparallel sheets, and no parallel sheets (Fig 2E). Taken together, these data demonstrate that the *K. kingae* PilC1 and PilC2 proteins are adhesins and have different binding affinities and distinct global protein structures.

Table 1. Strains and plasmids used in this study.

Strain or Plasmid	Description	Reference or Source
E. coli strains		
DH5α	*E. coli* F$^-$ ϕ80d*lacZ*Δ*M15* Δ(*lacZYA-argF*)*U169 deoR recA1 endA1 hsdR17*(r_K^- m_K^+) *phoA supE441 thi-1 gyrA96 relA1*	[19]
XL-10 Gold	Tet^{r}Δ(*mcrA*)183 Δ(*mcrCB-hsdSMR-mrr*)*173 endA1 supE44 thi-1 recA1 gyrA96 relA1 lac* Hte [F′ *proAB lacI*^{q}*Z*Δ*M15* Tn*10* (Tetr) Amy Cam^r]	Agilent
BL21(DE3) omp8	*E. coli* B F$^-$ *dcm ompT hsdS*(r_B^- m_B^-) *gal* λ(DE3) Δ*lamB ompF*::Tn5 *ΔompA ΔompC*	[20]
K. kingae strains		
KK03	Naturally occurring spreading and corroding variant of septic arthritis clinical isolate 269–492	[21]
KK03 derivatives		
Δ*pilA1*	KK03 with either an *aphA3* or *tetM* marked *pilA1* deletion	[7] and this work
Δ*pilF*	KK03 with an *aphA3* marked *pilF* deletion	[17]
Δ*pilC1*	KK03 with a *tetM* marked *pilC1* deletion	[17]
Δ*pilC2*	KK03 with an unmarked *pilC2* deletion	This work
Δ*pilC1*Δ*pilC2*	KK03 with a *tetM* marked *pilC1* deletion and an unmarked *pilC2* deletion	This work
Δ*pilT*	KK03 with an *ermC* marked *pilT* deletion	[17]
Δ*pilC1*Δ*pilT*	KK03 with an *ermC* marked *pilT* deletion and an *tetM* marked *pilC1* deletion	This work
Δ*pilC2*Δ*pilT*	KK03 with an *ermC* marked *pilT* deletion and an unmarked *pilC2* deletion	This work
Δ*pilC1*Δ*pilC2*Δ*pilT*	KK03 with a *tetM* marked *pilC1* deletion, an unmarked *pilC2* deletion, and an *ermC* marked *pilT* deletion	This work
Δ*pilC2*-ErmPilC1	KK03 *pilC2* deletion strain with an *ermC* insertion upstream of WT *pilC1*	[17]
Δ*pilC2*-ErmPilC1$_{Cterm}$	KK03 Δ*pilC2*-ErmPilC1 with a deletion of the 5'-region of *pilC1*	This work
Δ*pilC1*-KanPilC2	KK03 *pilC1* deletion strain with an *aphA3* insertion immediately downstream of WT *pilC2*	[17]
Δ*pilC1*-KanPilC2$_{Cterm}$	KK03 Δ*pilC1*-KanPilC2 with a deletion of the 5'-region of *pilC2*	This work
Plasmids		
pET22b	Protein expression vector	MilliporeSigma
pET22b/PilC1	For expression of 6xHisPilC1	This work
pET22b/PilC2	For expression of 6xHisPilC2	This work
pET22b/PilC1$_{Nterm}$	For expression of 6xHisPilC1 N-terminal domain	This work
pET22b/PilC2$_{Nterm}$	For expression of 6xHisPilC2 N-terminal domain	This work
pFalcon2	Source of *aphA3* kanamycin resistance gene	[22]
pHSX*tetM*4	Source of *tetM* tetracycline resistance gene	[23]
pIDN4	Source of *ermC* erythromycin resistance gene	[24]
pUC19/Δ*pilA1*:*kan*	*pilA1* deletion construct with an *aphA3* marked *pilA1* deletion	[7]
pUC19/Δ*pilA1*:*tet*	*pilA1* deletion construct with a *tetM* marked *pilA1* deletion	This work
pUC19/Δ*pilC1*	*pilC1* deletion construct with a *tetM* marked *pilC1* deletion	[7]
pUC19/Δ*pilT*	*pilT* deletion construct with an *ermC* marked *pilT* deletion	[17]
pUC19/Erm*pilC1*	For introduction of *ermC* marked *pilC1* locus	[17]
pUC19/*pilC2*Kan	For introduction of *aphA3* marked *pilC2* locus	[17]
pUC19/Erm*pilC1*ΔNterm	Construct transformed into strain Δ*pilC2* to generate strain Δ*pilC2* PilC1$_{Cterm}$	This work
pUC19/*pilC2*ΔNtermKan	Construct transformed into strain Δ*pilC1* to generate strain Δ*pilC1* PilC2$_{Cterm}$	This work
pTrc99A/Δ*knh*:*aphA3*	*knh* deletion construct marked with an *aphA3* kanamycin resistance marker	This work
pTrc99A/Δ*knh*:*ermC*	*knh* deletion construct marked with an *ermC* erythromycin resistance marker	This work
pBAD18	Protein expression vector with arabinose-inducible promoter	[25]

(*Continued*)

Table 1. (Continued)

Strain or Plasmid	Description	Reference or Source
pBAD-*pilC1*	pBAD18 encoding recombinant PilC1 minus the signal peptide	This work
pHAT10	Protein expression vector for generating HAT-fusions	Takara Bio
pHAT10-*gapdh*	pHAT10 encoding the HAT-GAPDH fusion protein	This work

https://doi.org/10.1371/journal.ppat.1010440.t001

K. kingae PilC1, but not PilC2, mediates bacterial adherence to extracellular matrix proteins

Given the limited homology between PilC1 and PilC2, the observed differences in PilC1 and PilC2 binding affinities with epithelial cells, and the different PilC1 and PilC2 predicted protein structures, we wondered whether these proteins might have distinct adhesive specificities. As shown in Fig 3, WT strain KK03 showed substantial adherence to collagen I, collagen IV, laminin, and fibronectin. In contrast, the non-piliated Δ*pilA1* mutant was nonadherent to these extracellular matrix (ECM) proteins, demonstrating that adherence is pilus-mediated. To assess the role of PilC1 and PilC2, we examined the mutant strains expressing only PilC1 (KK03Δ*pilC2*) or only PilC2 (KK03Δ*pilC1*). As shown in Fig 3, these assays revealed that PilC1, but not PilC2, was capable of mediating adherence to collagen I, collagen IV, laminin, and fibronectin. Interestingly, adherence to collagen I, collagen IV, and laminin was significantly greater by strain KK03Δ*pilC2* than by the wild type strain, suggesting that PilC2 may

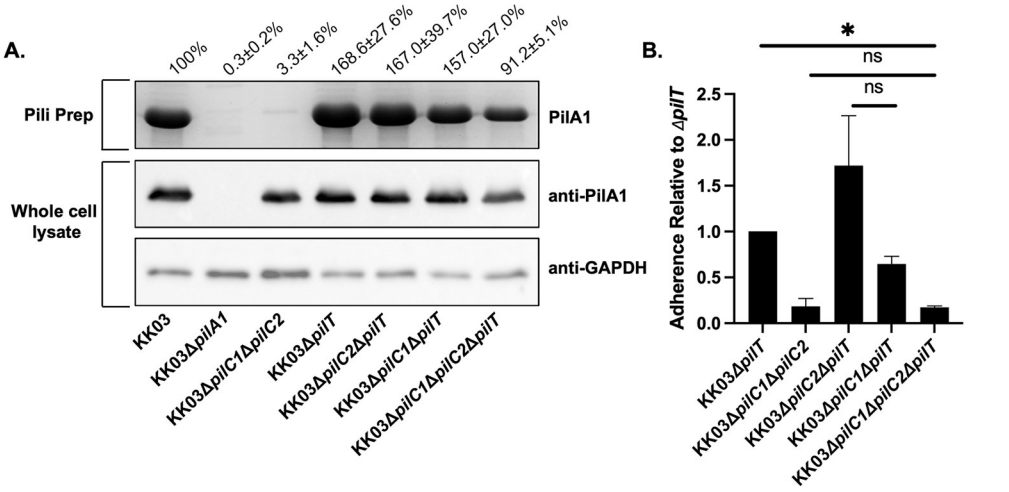

Fig 1. Deletion of retraction ATPase PilT restores surface piliation but not adherence in a *K. kingae* Δ*pilC1*Δ*pilC2* mutant strain. (A) Sheared pili fractions of strains KK03, KK03Δ*pilA1*, KK03Δ*pilC1*Δ*pilC2*, KK03Δ*pilT*, KK03Δ*pilC2*Δ*pilT*, KK03Δ*pilC1*Δ*pilT*, and KK03Δ*pilC1*Δ*pilC2*Δ*pilT* were boiled and separated using SDS-PAGE. For pili preps, the PilA1 pilin monomer band was stained with Coomassie blue. For whole cell lysates, the PilA1 pilin monomer band was detected by Western blot analysis using polyclonal antiserum GP65 [52] to PilA1. GAPDH was detected by Western blot analysis to control for total protein using polyclonal antiserum CHP-GP22. The values above the gel and blot images are densitometry measurements of the PilA1 band from the sheared pilus preparations (pili prep) gel that were normalized to the α-GAPDH band intensities and are expressed as a percentage of the band intensity of the wild type strain KK03. The densitometry values are listed ± standard error of the mean from three biological replicates, and representative gel and blot images are shown. (B) Strains KK03Δ*pilC1*Δ*pilC2*, KK03Δ*pilT*, KK03Δ*pilC2*Δ*pilT*, KK03Δ*pilC1*Δ*pilT*, and KK03Δ*pilC1*Δ*pilC2*Δ*pilT* were added to monolayers of Chang epithelial cells of HeLa origin and evaluated for adherence. Percent adherence was calculated based on the ratio of recovered bacteria to the inoculum. Error bars represent standard error of the mean, n = 3. * indicates significance of $P < 0.05$ as determined by a one-way ANOVA using Bonferroni correction for multiple comparisons. ns indicates no significance.

https://doi.org/10.1371/journal.ppat.1010440.g001

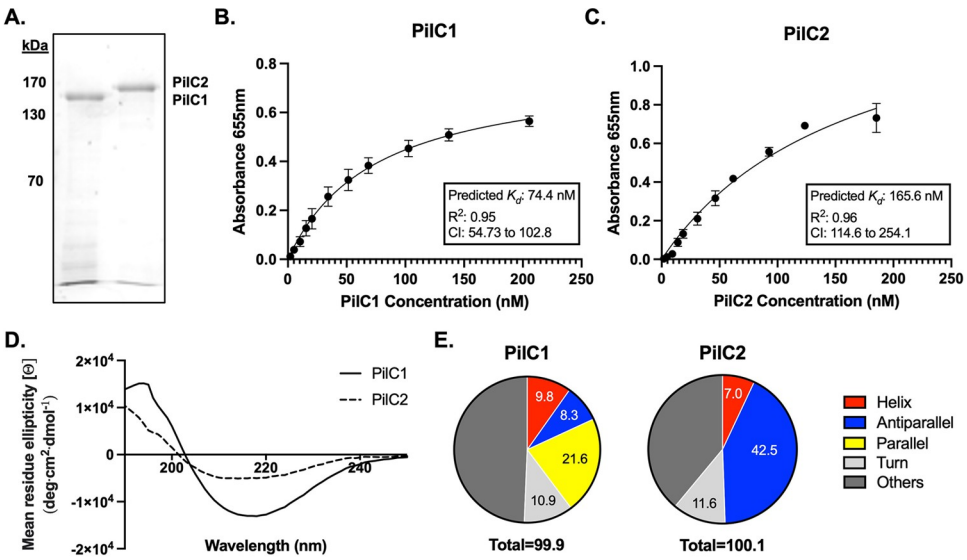

Fig 2. PilC1 and PilC2 are adhesins with distinct protein structures. (A) Recombinant PilC1 and PilC2 were purified and separated on a 7.5% SDS PAGE gel and stained with Coomassie blue. Proteins were added to monolayers of Chang epithelial cell of HeLa origin at increasing concentrations in 50 mM Tris-HCl, pH 8.5. (B, C) Adherence was detected by ELISA using polyclonal antiserum CHP-GP7 for PilC1 (B) or GP103 for PilC2 (C) and a secondary anti-guinea pig antibody conjugated to horseradish peroxidase (HRP). Non-linear regressions were fit using the GraphPad Prism one site specific binding model fit to total data from 3 independent runs, and the K_d was calculated based on the regression. Error bars represent standard error of the mean, n = 3. (D, E) Circular dichroism was carried out on purified PilC1 and PilC2 (D) and the resultant spectra were used to predict protein secondary structures (E). The CD spectra are representative graphs of three independent analyses carried out on different batches of purified protein.

https://doi.org/10.1371/journal.ppat.1010440.g002

interfere with PilC1-mediated binding. These results demonstrate that PilC1 is capable of binding to ECM proteins and establish that PilC1 and PilC2 have distinct binding specificities.

The *K. kingae* PilC1 and PilC2 C-terminal domains promote production of pilus fibers that lack adhesive activity

Previous work on the *P. aeruginosa* PilY1 protein established that the PilY1 C-terminal domain has a β-propeller fold and plays a critical role in *P. aeruginosa* type IV pilus assembly [26]. To localize the adhesive regions of PilC1 and PilC2, we generated deletion constructs lacking the N-terminal domains but containing intact C-terminal β-propeller folds (KK03Δ*pilC2*-ErmPilC1$_{Cterm}$ and KK03Δ*pilC1*-KanPilC2$_{Cterm}$) based on modeling with Phyre2 software [27] (S1 Fig). We hypothesized that the strains expressing only the C-terminal region of PilC1 or PilC2, in the absence of the other PilC, would still produce type IV pili but that these fibers would not be able to mediate adherence due to lack of the adhesive N-terminal region. Strains KK03Δ*pilC2*-ErmPilC1 and KK03Δ*pilC1*-KanPilC2, which contain an antibiotic marker upstream of the wild-type *pilC1* gene or downstream of the *pilC2* gene, respectively, were used as controls when evaluating the phenotypes of strains KK03Δ*pilC2*-ErmPilC1$_{Cterm}$ and KK03Δ*pilC1*-KanPilC2$_{Cterm}$. As shown in Fig 4A, piliation was reduced in strain KK03Δ*pilC2*-ErmPilC1 compared to the parent strain KK03Δ*pilC2*, indicating that the erythromycin resistance marker upstream of *pilC1* has a negative impact on pili levels. However, comparison of strains KK03Δ*pilC2*-ErmPilC1 and KK03Δ*pilC2*-ErmPilC1$_{Cterm}$ revealed similar piliation levels, indicating that the PilC1$_{Cterm}$ fragment is able to promote piliation at levels equivalent to full-length PilC1. Similarly, comparison of strain KK03Δ*pilC1*-KanPilC2 with strain KK03Δ*pilC1*-KanPilC2$_{Cterm}$ revealed equivalent levels of piliation, indicating that

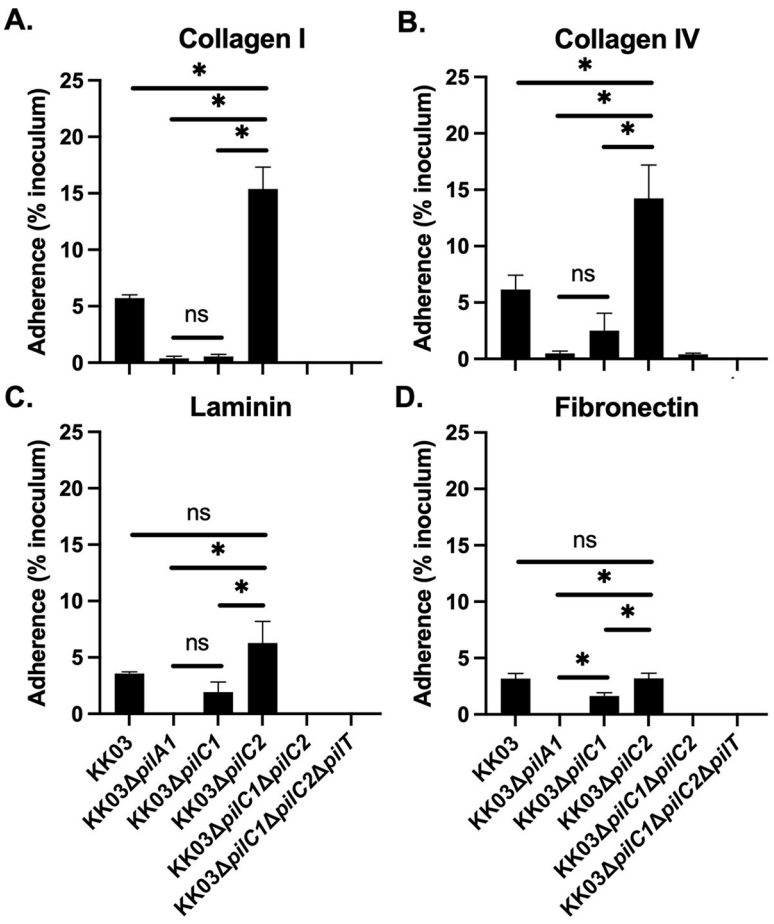

Fig 3. PilC1, but not PilC2, mediates *K. kingae* adherence to extracellular matrix. (A-D) Strains KK03, KK03Δ*pilA1*, KK03Δ*pilC1*, KK03Δ*pilC2*, KK03Δ*pilC1*Δ*pilC2*, and KK03Δ*pilC1*Δ*pilC2*Δ*pilCT* strains were added to plates coated with collagen I (A), collagen IV (B), laminin (C), or fibronectin (D) and evaluated for adherence. Percent adherence was calculated based on the ratio of recovered bacteria to the inoculum. Error bars represent standard error of the mean, n = 3. * indicates significance of $P < 0.05$ as determined by a one-way ANOVA using Bonferroni correction for multiple comparisons. ns indicates no significance.

https://doi.org/10.1371/journal.ppat.1010440.g003

the PilC2 C-terminal domain is also able to promote similar piliation levels as full-length PilC2. Despite the presence of pili, these strains were non-adherent in assays with cultured Chang cells of HeLa origin (Fig 4B and 4C), suggesting that the N-terminal domains of PilC1 and PilC2 are critical for adhesive activity. These results indicate that the C-terminal domains of PilC1 and PilC2 are sufficient for pilus assembly and suggest that the N-terminal domains of PilC1 and PilC2 harbor adhesive activity.

The *K. kingae* PilC1 and PilC2 N-terminal domains bind to epithelial cell monolayers

To obtain definitive evidence that the adhesive activity of PilC1 and PilC2 resides in the N-terminal domains of these proteins, we purified recombinant truncated 6X histidine-tagged PilC1 and PilC2 proteins corresponding to the N-terminal domains, lacking the predicted β-propeller region (Figs 5A and S1). As shown in Fig 5B, the PilC1 N-terminal domain exhibited saturable binding with a predicted K_d of 88.4 nM, comparable to the K_d of full-length PilC1 (74.4 nM). Similarly, as shown in Fig 5C, the PilC2 N-terminal domain displayed saturable

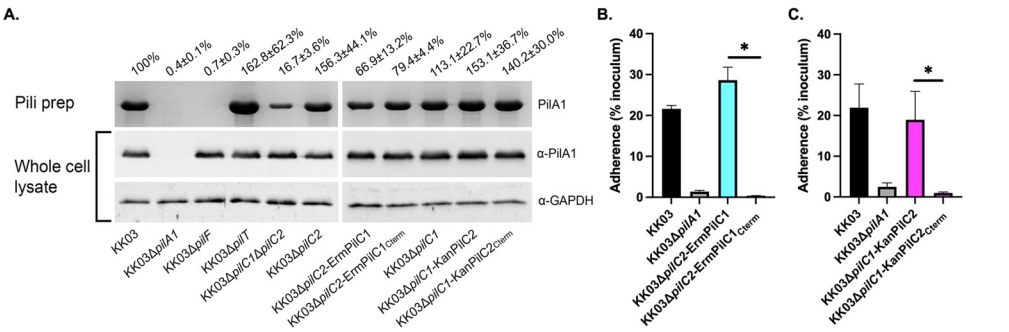

Fig 4. The PilC1 and PilC2 C-terminal domains promote production of pilus fibers that lack adhesive activity. (A) Sheared pili fractions or whole cell sonicates of strains KK03, KK03Δ*pilA1*, KK03Δ*pilF*, KK03Δ*pilT*, KK03Δ*pilC1*Δ*pilC2*, KK03Δ*pilC2*, KK03Δ*pilC2*-ErmPilC1, KK03Δ*pilC2*-ErmPilC1$_{Cterm}$, KK03Δ*pilC1*, KK03Δ*pilC1*-KanPilC2, and KK03Δ*pilC1*-KanPilC2$_{Cterm}$ were boiled and separated using SDS-PAGE. KK03Δ*pilF* lacks the PilF assembly ATPase and does not assemble PilA1 into pilus fibers. For pili preps, the PilA1 pilin monomer band was stained with Coomassie blue. For whole cell lysates, the PilA1 pilin monomer band was detected by Western blot analysis using polyclonal antiserum GP65 [52] to PilA1. GAPDH was detected by Western blot analysis to control for total protein using polyclonal antiserum CHP-GP22. The values above the gel and blot images are densitometry measurements of the PilA1 band from the sheared pilus preparations (pili prep) gel that were normalized to the α-GAPDH band intensities and are expressed as a percentage of the band intensity of the wild type strain KK03. The densitometry values are listed ± standard error of the mean from three biological replicates, and representative gel and blot images are shown. (B, C) Strains KK03, KK03Δ*pilA1*, KK03ErmΔ*pilC2*-PilC1, KK03Δ*pilC2*-ErmPilC1$_{Cterm}$, KK03Δ*pilC1*-KanPilC2, and KK03Δ*pilC1*-KanPilC2$_{Cterm}$ were added to monolayers of Chang epithelial cell of HeLa origin and evaluated for adherence. Percent adherence was calculated based on the ratio of recovered bacteria to the inoculum. Error bars represent standard error of the mean, n = 3. Cyan color denotes strains expressing either full-length PilC1 or the C-terminal region of PilC1 only. Magenta color denotes strains expressing either full-length PilC2 or the C-terminal region of PilC2 only. *indicates significance of $P < 0.05$ as determined by a one-way ANOVA using Bonferroni correction for multiple comparisons.

https://doi.org/10.1371/journal.ppat.1010440.g004

binding with a predicted K_d of 137.3 nM, comparable to the K_d of full-length PilC2 (165.6 nM). Based on CD spectroscopy (Fig 5D and 5E), the PilC1 N-terminal domain was predicted to contain 16.1% helices, 8.8% antiparallel sheets, 10.6% parallel sheets, and 13.6% turns, while the PilC2 N-terminal domain was predicted to contain 13.8% helices, 36.4% antiparallel sheets, 11.3% turns, and less than 2% parallel sheets. These data demonstrate that the PilC1 and PilC2 N-terminal domains harbor adhesive activity and appear to have distinct structures.

The PilC1 and PilC2 C-terminal domains are not sufficient for twitching motility but support transformation

To begin to localize other PilC1- and PilC2-mediated functions, we examined twitching motility in strains KK03Δ*pilC2*-ErmPilC1$_{Cterm}$ and KK03Δ*pilC1*-KanPilC2$_{Cterm}$. As shown in Fig 6A, compared to strain KK03Δ*pilC2*-ErmPilC1, strain KK03Δ*pilC2*-ErmPilC1$_{Cterm}$ was devoid of twitching motility, similar to the non-piliated Δ*pilA1* mutant. Compared to strain KK03Δ*pilC1*-KanPilC2, strain KK03Δ*pilC1*-KanPilC2$_{Cterm}$ was also devoid of twitching motility. These results suggest that the C-terminal domains of PilC1 and PilC2 are not sufficient for promoting twitching motility, localizing this activity to either the N-terminal domains or to regions in both the N-terminal and the C-terminal domains.

Twitching motility requires sequential pilus extension, adhesion to a substrate, and retraction. To determine if the defect in twitching motility in KK03Δ*pilC2*-ErmPilC1$_{Cterm}$ and KK03Δ*pilC1*-KanPilC2$_{Cterm}$ was due to a defect in pilus retraction, we examined natural transformation in these strains, recognizing that natural transformation requires pilus retraction in other systems [28]. The WT strain exhibited transformation efficiencies ranging from 0.3% to 1.5%, normalized to 1.0 in Fig 6B. As expected, the non-piliated Δ*pilA1* mutant and the

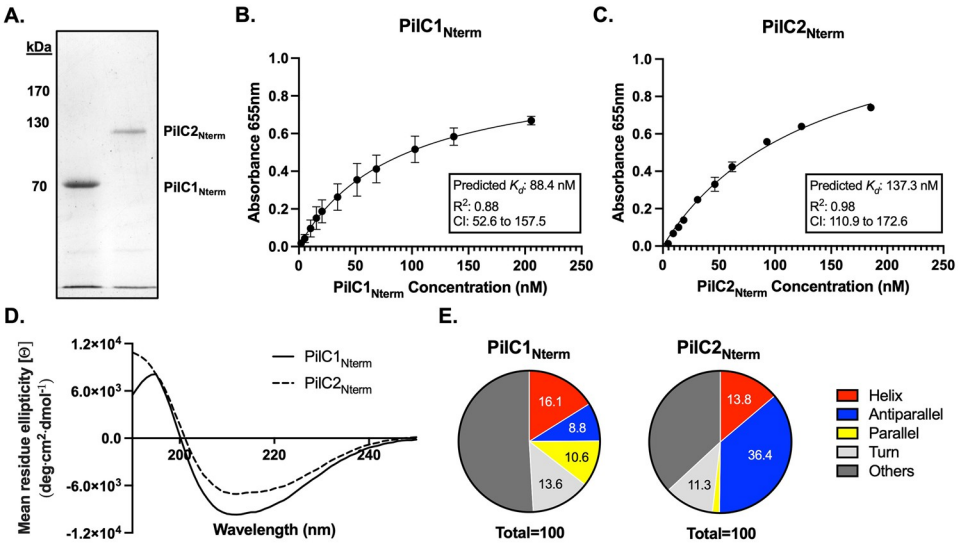

Fig 5. The PilC1 and PilC2 N-terminal domains bind to epithelial cell monolayers. (A) Recombinant PilC1 N-terminal domain ($PilC1_{Nterm}$) and PilC2 N-terminal domain ($PilC2_{Nterm}$) were purified and separated on a 7.5% SDS PAGE gel and stained with Coomassie blue. (B, C) Proteins were added to monolayers of Chang epithelial cells of HeLa origin at increasing concentrations in 50 mM Tris-HCl, pH 8.5. Adherence was detected by ELISA using polyclonal antiserum CHP-R1 for $PilC1_{Nterm}$ (B) or GP103 for $PilC2_{Nterm}$ (C) and a secondary anti-rat or anti-guinea pig antibody conjugated to HRP. Non-linear regressions were fit using the GraphPad Prism one site specific binding model fit to total data from 3 independent runs, and the K_d was calculated based on the regression. Error bars represent standard error of the mean, n = 3. (D, E) Circular dichroism was carried out on purified $PilC1_{Nterm}$ and $PilC2_{Nterm}$ (D) and the resultant spectra were used to predict protein secondary structures (E). The CD spectra are representative graphs of three independent analyses carried out on different batches of purified protein.

https://doi.org/10.1371/journal.ppat.1010440.g005

retraction-deficient Δ*pilT* mutant were completely non-transformable. Strain KK03Δ*pilC1*Δ-*pilC2* was capable of low but measurable levels of transformation, while strains KK03Δ*pilC2*-ErmPilC1 and KK03Δ*pilC1*-KanPilC2 displayed wild type levels of transformation, suggesting that the presence of either PilC1 or PilC2 is sufficient for wild type transformation efficiency. While strain KK03Δ*pilC*1-KanPilC2$_{Cterm}$ displayed wild type transformation efficiency, strain KK03Δ*pilC2*-ErmPilC1$_{Cterm}$ exhibited a statistically significant decrease in transformation efficiency when compared to KK03Δ*pilC2*-ErmPilC1. This lower level of transformation was above the level observed for strain KK03Δ*pilC1*Δ*pilC2*, indicating that the PilC1 C-terminal domain promotes transformation and that full transformation efficiency requires additional sequence N-terminal to the C-terminal domain fragment. Taken together, these data indicate that the PilC1 and PilC2 C-terminal domains are sufficient for retraction, and thus the lack of twitching motility in KK03Δ*pilC2*-ErmPilC1$_{Cterm}$ and KK03Δ*pilC1*-KanPilC2$_{Cterm}$ is not a consequence of absent pilus retraction.

Discussion

In this study we examined the role of the *K. kingae* PilC1 and PilC2 proteins in *K. kingae* adherence. Using purified full-length and truncated PilC1 and PilC2, we established that PilC1 and PilC2 are adhesins, with the adhesive activity located in the N-terminal domains of these proteins. Using deletion constructs, we found that PilC1-mediated and PilC2-mediated twitching motility requires the N-terminal domains. In contrast, our results indicate that the C-terminal domains of PilC1 and PilC2 are sufficient for promoting pilus assembly and natural transformation, although the PilC1 C-terminal domain is not sufficient for wild type transformation efficiency.

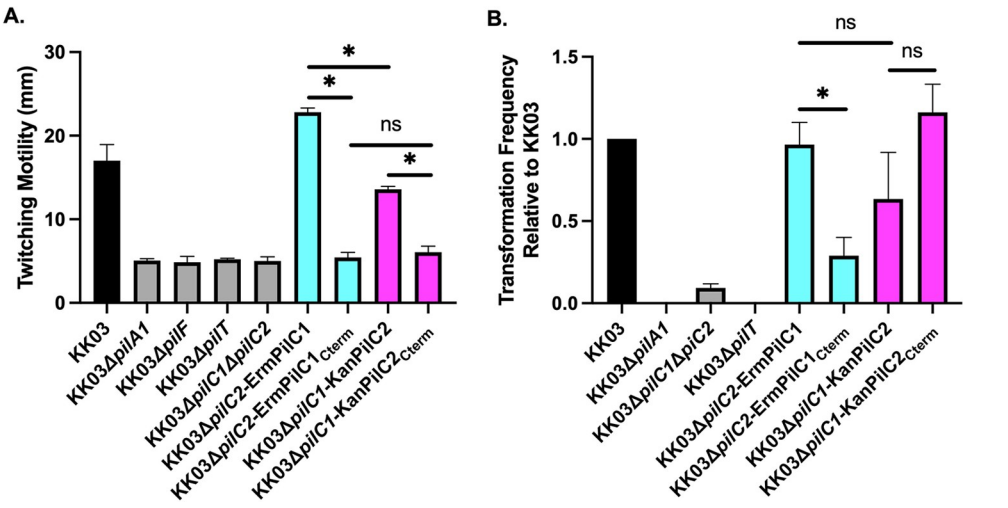

Fig 6. The PilC1 and PilC2 C-terminal domains are not sufficient for twitching motility but promote *K. kingae* natural transformation. (A) For strains KK03, KK03Δ*pilA1*, KK03Δ*pilF*, KK03Δ*pilT*, KK03Δ*pilC1*Δ*pilC2*, KK03Δ*pilC2*-ErmPilC1, KK03Δ*pilC2*-ErmPilC1$_{Cterm}$, KK03Δ*pilC1*-KanPilC2, and KK03Δ*pilC1*-KanPilC2$_{Cterm}$, the zone of twitching motility was stained with crystal violet and was quantified by measuring the diameter of bacterial spread. (B) Natural transformation was measured for strains KK03, KK03Δ*pilA1*, KK03Δ*pilC1*Δ*pilC2*, KK03Δ*pilT*, KK03Δ*pilC2*-ErmPilC1, KK03Δ*pilC2*-ErmPilC1$_{Cterm}$, KK03Δ*pilC1*-KanPilC2, and KK03Δ*pilC1*-KanPilC2$_{Cterm}$. Transformation frequency was calculated based on the ratio of recovered bacteria to inoculum. Error bars represent standard error of the mean, n = 3. Cyan color denotes strains expressing either full-length PilC1 or the C-terminal region of PilC1 only. Magenta color denotes strains expressing either full-length PilC2 or the C-terminal region of PilC2 only. *indicates significance of $P < 0.05$ as determined by a one-way ANOVA using Bonferroni correction for multiple comparisons. ns indicates no significance.

https://doi.org/10.1371/journal.ppat.1010440.g006

Earlier studies suggested that the *K. kingae* PilC1 and PilC2 proteins might be the adhesive components of the pilus, as expression of either the PilC1 or PilC2 protein is required for bacterial adherence to epithelial cells [7]. In this work, we found that deletion of the PilT retraction ATPase restored production of *K. kingae* surface fibers in the absence of a functional PilC protein but did not restore adherence. Furthermore, we observed that purified PilC1 and PilC2 were capable of binding to epithelial cell monolayers to saturating levels, providing strong evidence that these proteins are adhesins that interact with epithelial cells in a receptor-mediated process. Interestingly, the predicted K_d measurements of the *K. kingae* PilC1 and PilC2 N-terminal domains mimicked results with the full-length proteins, supporting the conclusion that full adhesive activity resides in the N-terminal domains [16].

Adhesins expressed by host-adapted bacteria commonly bind to extracellular matrix (ECM) components. Heiniger *et al*. showed that *P. aeruginosa* preferentially binds to the exposed basolateral cell surface of injured polarized epithelial cells in a PilY1-dependent manner [13]. As ECM proteins are located at the basolateral side of epithelial cells in the basement membrane and connective tissue, they are well positioned to serve as targets for bacterial adherence when there is damage to the epithelium. In this report, we demonstrate that *K. kingae* PilC1, but not PilC2, mediates bacterial adherence to ECM proteins. During the *K. kingae* pathogenic process, damage to the epithelial surface mediated by the *K. kingae* RTX toxin [21] or viral infection [29–32] may promote bacterial access to the basement membrane, where PilC1 may bind to ECM proteins, potentially facilitating invasive disease.

Our studies examining adherence to ECM proteins establish that the *K. kingae* PilC1 and PilC2 proteins have distinct binding specificities, consistent with the limited homology between PilC1 and PilC2 and the different global structures as assessed by CD spectroscopy. Interestingly, the *N. meningitidis* PilC1 and PilC2 proteins also have distinct binding

specificities, despite the fact that these proteins are highly homologous. In particular, *N. meningitidis* PilC1 has been demonstrated to promote meningococcal adherence to HEC-1-B, ME180, and HUVEC cell lines, while PilC2 promotes adherence only to ME180 cells [33,34].

It is notable that *K. kingae* PilC1-mediated adherence to ECM proteins was increased in the absence of PilC2, similar to our earlier observation that PilC1-mediated twitching motility was increased in the absence of PilC2 [17]. We have established that PilC1 and PilC2 production is not affected by the presence or the absence of the other protein (S2 Fig), suggesting that changes in expression cannot account for the differences in the phenotypes observed. One possibility is that PilC2 obscures PilC1 along the pilus and interferes with PilC1 interaction with its receptor. Another possibility is that PilC1 localization along the pilus is affected when PilC2 is eliminated. A third possibility is that PilC1 and PilC2 interact with each other and modify the function of each other.

The PilC family of proteins share a predicted C-terminal β-propeller fold domain. This fold was first identified when the C-terminal region of the *P. aeruginosa* PilY1 protein was crystallized [26], revealing a calcium-binding motif that is present in the β-propeller region of multiple PilC proteins [16,17,26,35]. Orans *et al*. showed that prevention of calcium-binding resulted in a defect in surface piliation and twitching motility, while mimicking the charge of a bound calcium ion produced an abundance of non-functional surface pili [26], suggesting a role for this domain in pilus biogenesis and retraction. Porsch *et al*. demonstrated that the *K. kingae* PilC1 and PilC2 calcium-binding motifs promoted twitching motility [17]. In this study, we observed that the C-terminal domain of *K. kingae* PilC1 and PilC2 was sufficient for promoting surface piliation, consistent with a role for the C-terminal domain in supporting pilus dynamics.

Studies in gram-negative bacteria have shown that T4P components and PilC proteins promote natural competence for transformation [28,36–38]. Because the expression of at least one PilC protein is required for surface piliation, ascertaining whether the proteins promote DNA uptake by promoting piliation or through another mechanism has been a challenge. KK03Δ*pilC2*-ErmPilC1$_{Cterm}$ displays reduced transformation efficiency compared to strain KK03Δ*pilC2*-ErmPilC1 despite expressing similar levels of pili (Fig 4A), suggesting that factors beyond piliation level influence transformation efficiency. Other possible mechanisms of PilC protein involvement include direct binding of DNA or influencing other known competence proteins such as the pilus-associated ComP, which binds to DNA [39,40], or the periplasmic ComE or ComA, which function to promote DNA uptake and translocation [41–47]. As PilC1 and PilC2 localize to surface pili (S2 Fig), it is feasible that they may interact with ComE or ComA in the periplasm to modulate DNA translocation, or ComP along the pilus fiber to modulate DNA binding. The transformation defect observed in KK03Δ*pilC2*-ErmPilC1$_{Cterm}$ but not KK03Δ*pilC1*-KanPilC2$_{Cterm}$ raises the possibility that PilC1 and PilC2 have different functions during transformation. The PilC1 N-terminal region may function in combination with the C-terminal region to promote transformation, while the PilC2 C-terminal region may function alone to promote transformation using a distinct mechanism.

Twitching motility is believed to be carried out by sequential T4P extension, adhesion to a substrate, and PilT-mediated retraction of the adhering pilus fibers, which exert a pulling force allowing the bacteria to move along a surface [28,48–51]. In PilC-containing bacteria, at least one functional PilC protein is required for a twitching phenotype [10,17,26]; however, it remains to be determined if the PilC proteins promote twitching motility by promoting adherence, by regulating the pilus extension/retraction dynamic, or both. Strains KK03Δ*pilC2*-ErmPilC1$_{Cterm}$ and KK03Δ*pilC1*-KanPilC2$_{Cterm}$ produce retractile pilus fibers, as evidenced by their natural transformation. Despite being retractile, the present fibers are unable to promote

bacterial adherence to epithelial cells. For this reason, the defect observed in twitching motility is likely due to a defect in adherence, rather than a defect in pilus retraction.

Our data demonstrate that *K. kingae* PilC1 and PilC2 differentially promote *K. kingae* adherence using the N-terminal domains to directly interact with epithelial cells and the C-terminal domains to promote surface piliation. Future studies should elucidate the specific adhesive motifs in PilC1 and PilC2 and should address whether PilC1 and PilC2 interact with each other to modulate type IV pilus-mediated phenotypes.

Methods

Generation of *K. kingae* mutants

K. kingae gene disruptions and mutations were generated as described previously [7,17,52]. Plasmid-based disruption and truncation constructs were generated in *E. coli*, linearized, and introduced into *K. kingae* using natural transformation of linearized plasmid DNA followed by selection for mutants on chocolate agar plates with the appropriate antibiotic. Mutations were confirmed by genomic DNA preparation of putative mutant strains followed by PCR amplification and evaluation by Sanger sequencing.

To generate the unmarked KK03Δ*pilC2* mutant, the plasmid pUC19/Δ*pilC2* [17] lacking a resistance cassette was transformed into the kanamycin-marked strain KK03Δ*pilC2* using the spot transformation technique [53], and patch plating was used to screen for the loss of kanamycin resistance. To generate strain KK03Δ*pilC1*Δ*pilC2*, linearized pUC19/Δ*pilC1* [7] was introduced into KK03Δ*pilC2* and transformants were recovered by selection on chocolate agar with 2 μg/ml tetracycline. To generate strain KK03Δ*pilC2*Δ*pilT*, linearized pUC19/Δ*pilT* [17] DNA was introduced into strain KK03Δ*pilC2* and transformants were recovered by selection on chocolate agar with 1 μg/ml erythromycin. To generate strain KK03Δ*pilC1*Δ*pilT*, linearized pUC19/Δ*pilT* [17] DNA was introduced into strain KK03Δ*pilC1* [17], as described above. To generate strain KK03Δ*pilC1*Δ*pilC2*Δ*pilT*, linearized pUC19/Δ*pilT* [17] DNA was introduced into strain KK03Δ*pilC1*Δ*pilC2* as described above. For pUC19/Δ*pilA1*:*tet*, the *aphA3* kanamycin resistance cassette in pUC19/Δ*pilA1*:*kan* [7] was excised as a MluI-fragment and replaced with a *tetM* tetracycline resistance cassette. For strain KK03Δ*pilA1*, linearized plasmid pUC19/Δ*pilA1*:tet DNA was introduced into KK03 and transformants were recovered by selection on chocolate agar with 2 μg/ml tetracycline.

To generate strain KK03Δ*pilC2*-ErmPilC1$_{Cterm}$, site-directed mutagenesis using primers C1ΔNterm_mut_sense and C1ΔNterm_mut_anti (see Table 2 for the primer sequences used in this study) and the QuikChange II XL Site-directed mutagenesis kit (Agilent, Santa Clara, CA) was used to delete sequence encoding amino acids 32–438, using plasmid pUC19/Erm-*pilC1* [17] as the template. The C-terminal domains were designated as the region of the proteins encompassing the predicted β-propeller fold based on modeling with Phyre2 software [27], and the N-terminal regions were defined as the polypeptide excluding the signal sequence and the predicted β-propeller fold. The resulting construct, pUC19/Erm*pilC1*ΔNterm, which contains an erythromycin resistance marker upstream of the *pilC1* promoter region and the PilC1 signal sequence fused in-frame to the C-terminal domain, was linearized and transformed into strain KK03Δ*pilC2*, generating strain KK03Δ*pilC2*-ErmPilC1$_{Cterm}$. To generate strain KK03Δ*pilC1*-KanPilC2$_{Cterm}$, Gibson assembly was employed using DNA fragments amplified with Q5 Hi-Fidelity Master Mix with primer pairs *pilC2*up_F and *pilC2*up_R (Table 2) (using KK03 genomic DNA as template) and *pilC2*downKan_F and *pilC2*down-Kan_R (using KK03Δ*pilC1*-KanPilC2 [17] genomic DNA as the template) and EcoRI-digested pUC19. The resulting plasmid, pUC19/*pilC2*ΔNtermKan, which contains sequence encoding the PilC2 signal sequence fused in-frame to sequence encoding the C-terminal domain and a

Table 2. Primers used in this study.

Primer	Sequence (5' → 3')
GibCytoC1F	TTTAAGAAGGAGATATACATATGCATCATCACCATCACCAC
GibCytoC1R	CAGTGGTGGTGGTGGTGGTGCTCGAGTTAGAAAATCTCACGCCAAG
GibCytoC2F	CTTTAAGAAGGAGATATACATATGCATCATCACCATCACCACAACAATACCCCTTTTTCTGATTC
GibCytoC2R	AGTGGTGGTGGTGGTGGTGCTTAGAAAATCTCGCGCCAAG
CNtermF	CTTTAAGAAGGAGATATACATATGCATCATCACCATCACCAC
C1NtermR	AGTGGTGGTGGTGGTGGTGCTTATTGCGCAATGCCATTTTTAC
C2NtermR	AGTGGTGGTGGTGGTGGTGCTTAGCTAATATTGGCAGATG
C1ΔNterm_mut_sense	GCGACAATGGCGGCTGATGTACAAAAAGCGTACTATT
C1ΔNterm_mut_anti	AATAGTACGCTTTTTGTACATCAGCCGCCATTGTCGC
*pilC2*up_F	TTGTAAAACGACGGCCAGTGCACAACAGAGTAACACCATG
*pilC2*up_R	TGCCATCTTCGTTTTCTGCTTGTGCATAAAAAG
*pilC2*downKan_F	AGCAGAAAACGAAGATGGCAGAAAATTCCG
*pilC2*downKan_R	ATCCCCGGGTACCGAGCTCGGGTAATCCAGCACGAGATTTG
pBAD*pilC1*_F	CGTTTTTTTGGGCTAGCGGTGAGTAGTATGAGTCTTAAATATAAAAAATATAATTG
pBAD*pilC1*_R	CGGGTACCGAGCTCGATTTTTGTGAATACAGGTTCTG
*gapdh*_F	ACGTGTCGACATGAGCGTTAAAGTAGCCATTAAC
*gapdh*_R	AGCTGAATTCATAATAATCAAAGCAGCCTGCAC

https://doi.org/10.1371/journal.ppat.1010440.t002

kanamycin-resistance marker downstream of the *pilC2* ORF, was linearized and transformed into strain KK03Δ*pilC1*, generating strain KK03Δ*pilC1*-KanPilC2$_{Cterm}$. A schematic representation of the *pilC1* and *pilC2* loci in the panel of mutants used in this study is shown in S3 Fig.

For the transformation efficiency experiments, the plasmid pTrc99a/*knh*:*tetM* [8] was modified by excising the *tetM* cassette as a ClaI fragment and inserting the *aphA3* kanamycin resistance cassette or the *ermC* erythromycin resistance cassette, generating pTrc99a/*knh*:*aphA3* and pTrc99a/*knh*:*ermC*, respectively.

Eukaryotic cell lines

Chang epithelial cells (Wong-Kilbourne derivative [D] of Chang conjunctiva, HeLa origin; ATCC CCL-20.2) were grown at 37˚C, 5% CO_2 in Modified Eagles' Medium (MEM) supplemented with 10% fetal bovine serum (FBS) and non-essential amino acids diluted 1:100, as described previously [21].

Generation of recombinant PilC1 and PilC2 constructs

Sequences corresponding to the ORFs of *pilC1* and *pilC2* lacking sequence encoding the predicted signal sequences were amplified from genomic DNA from either KK03 or KK03 producing 6X histidine-tagged PilC1 using Q5 High-Fidelity Master Mix (New England Biolabs, Ipswich, MA) with the primers GibCytoC1F and GibCytoC1R for PilC1 and GibCytoC2F and GibCytoC2R for PilC2. The signal sequence cleavage sites were predicted using SignalP [54,55]. The 6X histidine tag was placed at the N-terminus of the protein immediately following the predicted signal peptide cleavage site. The recombinant PilC1 full-length protein encompassed amino acids Asp_{35} – Phe_{1359}, and the recombinant PilC2 full-length protein encompassed amino acids Asn_{37} –Phe_{1502}. Gibson assembly was used to introduce sequence encoding 6X histidine-tagged PilC1 and PilC2 into the vector pET22b, generating pET22b-PilC1 and pET22b-PilC2, respectively. For PilC2 an N-terminal 6X histidine tag was added using primers GibCytoC2F and GibCytoC2R. The assembly reaction was carried out using the Gibson Assembly Master Mix (New England Biolabs)

according to the manufacturer's instructions, and the reaction was transformed into electrocompetent *E. coli* DH5α followed by the selection for transformants on LB agar with 100 μg/ml ampicillin. The plasmids were purified, and the constructs were confirmed using Sanger sequencing. The N-terminal regions of PilC1 and PilC2 were amplified from pET22b-PilC1 and pET22b-PilC2 using Q5 High-fidelity Master Mix with primers CNtermF and C1NtermR for PilC1 and CNtermF and C2NtermR for PilC2. The C-terminal domains were designated as the region of the proteins encompassing the predicted β-propeller fold based on modeling with Phyre2 software [27], and the N-terminal regions were defined as the polypeptide excluding the signal sequence and the predicted β-propeller fold. The amplified PilC1 N-terminal region encompassed amino acids Asp_{35} –Gln_{672}, while the PilC2 N-terminal region encompassed amino acids Asn_{37} – Ser_{1022}. Gibson assembly was used to introduce sequence encoding the 6X histidine-tagged PilC1 N-terminal region and the 6X histidine-tagged PilC2 N-terminal region into pET22b, generating pET22b-$PilC1_{Nterm}$ and pET22b-$PilC2_{Nterm}$, which were purified and confirmed using Sanger sequencing. The confirmed constructs were introduced into electrocompetent *E. coli* BL21 followed by selection for transformants on LB agar with 100 μg/ml ampicillin.

PilC1 and PilC2 protein purification

Overnight cultures of *E. coli* BL21 with either pET22b-PilC1, pET22b-PilC2, pET22b-$PilC1_{Nterm}$, or pET22b-$PilC2_{Nterm}$ were back-diluted 1:200 in LB broth with 100 μg/ml ampicillin. After reaching an OD_{600} of 0.4, gene expression was induced for 3 hours at 30˚C using 0.04 mM isopropyl β-D-1-thiogalactopyranoside (IPTG). Subsequently, the cultures were centrifuged at 6700 x g for 20 minutes, and the supernatant was discarded. The cell pellets were resuspended in 50 mM tris-HCl, 5 mM EDTA, and 10 mM NaCl at pH 8.0 at a ratio of 3 ml buffer to 1 gram of cells. AEBSF was added to a final concentration of 1 mM. For each 1 gram of cells, 0.8 mg of lysozyme was added. The solution was mixed and placed in a 37˚C water bath until viscous. The solution was sonicated 3 x at 25% amplitude for 30 seconds using a QSonica Q500 sonicator to shear DNA. The solution was centrifuged at 39,191 x g for 30 minutes, and the supernatant was discarded. The resulting pellets were resuspended in 20 mM Na_2HPO_4, 20 mM NaCl, 5 mM EDTA, and 25% sucrose at pH 7.2 at a ratio of 3 ml buffer to 1 gram of material. AEBSF was again added to a final concentration of 1 mM. Triton X-100 was added to a final concentration of 1%. The solution was mixed and centrifuged at 48,384 x g for 20 minutes, and the supernatant was discarded. The pellets were solubilized using 50 mM tris-HCl, 40 mM imidazole, 8 M urea, and 1mM β-mercaptoethanol at pH 8.0 (solubilization buffer) for several hours at 37˚C, adding more buffer until no more pellet would solubilize. The solubilized pellet was centrifuged at 48,384 x g for 20 minutes. The remaining supernatant was filtered using vacuum filtration through a 0.22 μM membrane, and the 6X histidine-tagged PilC1, PilC2, $PilC1_{Nterm}$, or $PilC2_{Nterm}$ was purified from the supernatant using affinity chromatography over an Ni-NTA agarose column. The 2 ml column bed volume was equilibrated with the solubilization buffer, and the supernatants were added to the column and incubated at room temperature on a rotator for 3 hours to facilitate protein-binding. The column was washed wth 20 ml of solubilization buffer. Proteins were eluted with 50 mM tris-HCl, 500 mM imidazole, 8 M urea, and 1 mM β-mercaptoethanol at pH 8.0. The samples were concentrated over a 100,000 Da molecular weight cutoff filter for PilC1 and PilC2 or a 50,000 Da molecular weight cutoff filter for $PilC1_{Nterm}$ and $PilC2_{Nterm}$. The samples were then dialyzed into 1 L 50 mM tris-HCl at pH 8.5 at 4˚C for 24 hours. The buffer was removed and replaced with 1 L fresh buffer, and samples were dialyzed at 4˚C for an additional 24 hours. The protein samples were stored at 4˚C in 50 mM Tris-HCl at pH 8.5.

Generation of polyclonal antisera

To generate a guinea pig antiserum to PilC1, the sequence encoding PilC1 minus the predicted signal peptide was amplified from KK03 genomic DNA with primers pBAD*pilC1*_F and pBAD*pilC1*_R and was cloned into KpnI-digested pBAD18 using Gibson assembly. The resulting plasmid pBAD-*pilC1* was transformed into electrocompetent DH5α, and gene expression was induced with 0.2% arabinose. The bacterial pellet was harvested and sonicated. After centrifugation, the insoluble fraction containing recombinant PilC1 was separated on a 7.5% SDS-PAGE gel and stained with Coomassie blue, and the PilC1 band was excised and sent to Cocalico Biologicals to immunize a guinea pig (CHP-GP7) according to their standard antiserum generation protocol. To generate a rat antiserum to PilC1, 6XHisPilC1 was used to immunize a rat (CHP-R1) at Cocalico Biologicals according to their standard antiserum generation protocol. To generate an antiserum to PilC2, a PilC2 fragment corresponding to amino acids 868–1502, generated as previously described [17], was used to immunize a guinea pig (GP103) at Cocalico Biologicals according to their standard antiserum generation protocol. To generate a rabbit polyclonal antiserum to the PilC1 N-terminal region, recombinant $PilC1_{Nterm}$ was used to immunize a rabbit (Rab128) at Cocalico Biologicals according to their standard antiserum generation protocol.

To generate an antiserum to the *K. kingae* glyceraldehyde phosphate dehydrogenase (GAPDH) protein, the full *gapdh* gene sequence (minus the start codon) was amplified using Q5 High-Fidelity Master Mix with primers *gapdh*_F and *gapdh*_R using KK03 genomic DNA as template. The resulting amplicon was digested with EcoRI and BamHI and ligated into EcoRI/BamHI-digested pHAT10, generating plasmid pHAT10-*gapdh*, encoding N-terminal histidine affinity tag (HAT)-tagged GAPDH. The plasmid was transformed into *E. coli* BL21 (DE3), and expression of the recombinant *gapdh* gene was induced with 0.4 mM IPTG for 3 hours at 30˚C. The resulting bacterial pellet was suspended in binding/wash buffer (20 mM sodium phosphate pH 7.4, 500 mM NaCl, 40 mM imidazole), sonicated, clarified via centrifugation at 20,000 x g for 20 min, and applied to a pre-equilibrated 5 ml HisTrap column (Cytiva, Marlborough, MA), using an AKTA Protein Purifier 10. After washing with 10 column volumes of binding/wash buffer, the bound protein was eluted with 20 mM sodium phosphate pH 7.4, 500 mM NaCl, 500 mM imidazole. The fractions containing the fusion protein were pooled, buffer exchanged and concentrated in 20 mM sodium phosphate pH 7.4, 500 mM NaCl using a 10,000 Da molecular weight cutoff filter, and then frozen at -80˚C. The purified fusion protein was then sent to Cocalico Biologicals for injection into a guinea pig (CHP-GP22) using their standard antiserum generation protocol. Reactivity of all antisera was assessed using Western blot analysis.

Cell-based protein-binding assays

Chang epithelial cells of HeLa origin were seeded into 96 well tissue culture-treated plates at a density of 3.24×10^4 cells per well, and the plates were incubated overnight for ~18 hours at 37˚C, 5% CO_2. The cells were then fixed with 2% glutaraldehyde in sodium phosphate buffer and washed 3x with Tris-buffered saline (TBS). The monolayers were blocked using 2% dry milk powder in phosphate-buffered saline (PBS) for 1.5 hours at 37˚C. Protein dilutions ranging from 1.85 nM to 205.55 nM were prepared in 50 mM Tris-HCl, pH 8.5. The blocking buffer was removed, and the diluted proteins were added to either tissue culture treated plates only or tissue culture treated plates coated with epithelial cell monolayers. Protein-loaded plates were incubated at 37˚C for 3 hours before being washed 4 x with PBS. Polyclonal antisera diluted 1:500 in 2% dry milk powder/PBS was added to the plates, which were incubated at 37˚C for 45 minutes and then washed 4 x with PBS. A secondary antibody conjugated to

horseradish peroxidase diluted 1:2000 in 2% dry milk powder/PBS was added to the plates, and plates were incubated at 37˚C for 45 minutes before being washed 4 x with PBS. Peroxidase substrate (3, 3', 5, 5'–Tetramethylbenzidine) was added to the plates, and the color change was measured at 655 nm after 11 minutes of development using a multimode plate reader. Non-specific protein adherence to the plate and antibody adherence to epithelial cells were subtracted from the total protein adherence detected to epithelial cell monolayers to generate specific binding data.

Circular dichroism

PilC1, PilC2, $PilC1_{Nterm}$, and $PilC2_{Nterm}$ proteins were diluted to a final concentration of 50 μg/ml in 16 mM tris-HCl, pH 8.5 and analyzed using a Jasco J-810 spectropolarimeter, using a 0.1 cm cuvette at a wavelength range of 250–190 nm. The spectropolarimeter was blanked using 16 mM Tris-HCl, pH 8.5 prior to taking measurements. The parameters were set to 1 nm data pitch, standard sensitivity, 1 s DIT, 1 nm bandwidth, immediate start mode, 20 nm/min scan speed, and 6 total accumulations. Spectra were converted to mean residue ellipticity to account for differences in the size of the proteins, and protein secondary structures were predicted using BeStSel [56,57].

Quantitative bacterial adherence assays

Quantitative adherence assays were performed as described previously [7,8,17,52]. For determining adherence levels, Chang epithelial cells of HeLa origin were seeded into 24-well tissue culture treated plates and incubated overnight at 37˚C, 5% CO_2. The cells were then fixed with 2% glutaraldehyde in 0.2 M sodium phosphate buffer pH 7.4 and washed 3 x with TBS. For determining adherence to extracellular matrix (ECM), BioCoat plates coated with either collagen I, collagen IV, fibronectin, or laminin were purchased from Corning (Corning, NY). The ECM plates were equilibrated at room temperature for one hour prior to inoculation. The bacteria were cultured on chocolate agar plates at 37˚C, 5% CO_2 for 18–20 hours, swabbed from the plate, and resuspended in brain heart infusion media (BHI) to an OD_{600} of 0.8. A volume of 10 μl of resuspended bacteria was added to 300 μl of prewarmed 37˚C MEM in 24-well tissue culture treated plates coated with either epithelial cell monolayers or ECM. The plates were incubated at 37˚C, 5% CO_2 for 25 minutes and were then washed 4 x with PBS to remove unbound bacteria. A volume of 100 μl 0.05% trypsin-EDTA was added to the plates, followed by incubation at 37˚C, 5% CO_2 for 20 minutes to facilitate bacterial recovery. The recovered bacteria were diluted and plated onto chocolate agar, and percent adherence was calculated based on the ratio of recovered bacteria to the inoculum.

Pilus preparations

Pilus preparations were performed using a large-scale method modified from the small-scale method described previously [17]. Bacteria were grown at 37˚C, 5% CO_2 for 20 hours on chocolate agar plates, swabbed from the plate, and resuspended in 12 ml PBS to an OD_{600} of 0.8. Samples were vortexed at full speed for 1 min and centrifuged at 4,000 x g for 30 min to pellet bacteria. A total of 10 ml of the bacteria-free supernatant was subjected to 20% ammonium sulfate precipitation on ice for 2 hours. Precipitated pili were collected via centrifugation at 20,000 x g for 20 min and resuspended in 1x SDS-PAGE loading buffer. Pilus preparations were separated on 15% SDS-PAGE gels, stained with Coomassie blue, and imaged with a Syngene G:Box system.

Densitometry analysis

To quantitate piliation levels, the PilA1 major pilin subunit band densities of Coomassie blue-stained pilus preparations and the Western blot GAPDH band densities of whole cell lysates (from the same bacterial pellet from which the pili were sheared for the pilus prepartions) were measured using ImageJ software [58,59]. The PilA1 band densities were divided by their matched GAPDH loading control band densities for normalization. The normalized values were then divided by the wild type KK03 normalized value to set wild type to 100% and compare all of the other strains to the wild type level. This analysis was completed for three independent biological replicates, and the average relative normalized PilA1 levels are presented ± standard error of the mean.

Transformation efficiency assays

Strains were suspended to an OD_{600} of 0.8 in BHI broth, and 250 μl of the bacterial suspension was added to wells of a 24-well plate. A total of 1.0 μg of plasmid DNA containing either a kanamycin or erythromycin resistant cassette in place of the *knh* gene, using a plasmid backbone previously used to generate a *knh* deletion via allelic exchange [8], was added to the bacterial suspension. The transformation mixture was left at room temperature for 30 minutes, followed by the addition of 250 μl of BHI/20% lysed horse blood. The mixture was incubated at 37˚C, 5% CO_2 for 2.5 hours to allow for bacterial recovery before plating on chocolate agar containing 50 μg/ml kanamycin or 1 μg/ml erythromycin. The plates were incubated at 37˚C, 5% CO_2 overnight, and transformant colony forming units (cfu) were then enumerated. Transformation efficiency was calculated based on the ratio of kanamycin-resistant or erythromycin-resistant transformed cfu relative to the inoculum cfu.

Twitching motility assays

Twitching motility assays were performed as described previously [17]. The strains were suspended to an OD_{600} of 0.8 in BHI. A 1 μl volume of the bacterial suspension was stab inoculated into the center of a chocolate agar motility plate (chocolate agar with 1% agar) to the plate-agar interface using a pipette tip. Plates were incubated at 37˚C, 5% CO_2 for three days. After three days the chocolate agar was removed, and the zone of bacterial spread at the plate-agar interface was stained with 0.1% crystal violet. The diameter of the crystal violet-stained bacterial spread was measured in millimeters.

Supporting information

S1 Fig. Schematic of full and truncated PilC1 and PilC2 proteins used in this study. PilC1, PilC1 C-terminal region ($PilC1_{Cterm}$), PilC2, and PilC2 C-terminal region ($PilC2_{Cterm}$) proteins expressed in *K. kingae* are shown with the included amino acids. Dashed boxes represent deleted regions of the protein. Black lines represent a fusion of the signal sequence with the C-terminal region. Black color represents the predicted signal sequence. The blue color represents the predicted PilC β- propeller domain. Recombinant PilC1 and PilC2 N-terminal proteins, expressed in *E. coli*, lack the signal sequence and are depicted as $PilC1_{Nterm}$ and $PilC2_{Nterm}$ in the diagram.
(TIF)

S2 Fig. PilC1 and PilC2 localize to surface pili. Sheared pili fractions of strains KK03, KK03Δ*pilA1*, KK03Δ*pilC1*, KK03Δ*pilC2*, KK03Δ*pilC1*Δ*pilC2*, and KK03Δ*pilC1*Δ*pilC2*Δ*pilT* were boiled and separated using SDS-PAGE. PilC1 was detected by Western blot analysis using polyclonal antiserum Rab128 to $PilC1_{Nterm}$, PilC2 was detected by Western blot analysis

using polyclonal antiserum GP103 to PilC2, and GAPDH was detected by Western blot analysis using polyclonal antiserum GP22 to GAPDH. The PilA1 pilin monomer band was stained with Coomassie blue.
(TIF)

S3 Fig. Cartoon representation of the *pilC1* and *pilC2* loci and *pilC1* and *pilC2* mutants used in this study. Strain KK03 (WT) produces PilC1 and PilC2, which are encoded by the *pilC1* and *pilC2* genes. Strain KK03Δ*pilC1*Δ*pilC2* contains a tetracycline resistance cassette in place of *pilC1* and an unmarked deletion of *pilC2* and does not produce PilC1 or PilC2. Strain KK03Δ*pilC2* contains an unmarked deletion of *pilC2* and produces full-length PilC1. Strains KK03Δ*pilC2*-ErmPilC1 and KK03Δ*pilC2*-ErmPilC1$_{Cterm}$ contain an unmarked deletion of *pilC2* and an erythromycin resistance cassette upstream of *pilC1* and produce full-length PilC1 and the C-terminal domain of PilC1, respectively. Strain KK03Δ*pilC1* contains a tetracycline resistance cassette in place of *pilC1* and produces full-length PilC2. Strains KK03Δ*pilC1*-KanPilC2 and KK03Δ*pilC1*-KanPilC2$_{Cterm}$ contain a tetracycline resistance cassette in place of *pilC1* and a kanamycin resistance cassette downstream of *pilC2* and produce full-length PilC2 and the C-terminal domain of PilC2, respectively. SS represents the predicted signal sequence. Cyan color denotes strains producing either full-length PilC1 or the C-terminal region of PilC1; magenta color denotes strains producing either full-length PilC2 or the C-terminal region of PilC2. The dashed lines indicate a deletion. Tet^R, Kan^R, and Erm^R indicate tetracycline, kanamycin, and erythromycin resistance cassettes, respectively.
(TIF)

Author Contributions

Conceptualization: Alexandra L. Sacharok, Eric A. Porsch, Joseph W. St. Geme, III.

Data curation: Alexandra L. Sacharok, Eric A. Porsch, Taylor A. Yount, Orlaith Keenan.

Formal analysis: Alexandra L. Sacharok, Eric A. Porsch, Joseph W. St. Geme, III.

Funding acquisition: Joseph W. St. Geme, III.

Investigation: Alexandra L. Sacharok, Eric A. Porsch, Taylor A. Yount, Orlaith Keenan.

Methodology: Alexandra L. Sacharok, Eric A. Porsch, Joseph W. St. Geme, III.

Project administration: Alexandra L. Sacharok, Eric A. Porsch, Joseph W. St. Geme, III.

Supervision: Alexandra L. Sacharok, Eric A. Porsch, Joseph W. St. Geme, III.

Validation: Joseph W. St. Geme, III.

Visualization: Alexandra L. Sacharok, Eric A. Porsch.

Writing – original draft: Alexandra L. Sacharok, Eric A. Porsch, Joseph W. St. Geme, III.

Writing – review & editing: Alexandra L. Sacharok, Eric A. Porsch, Joseph W. St. Geme, III.

References

1. Yagupsky P. *Kingella kingae*: From medical rarity to an emerging paediatric pathogen. Lancet Infectious Diseases. 2004; 4: 358–367. https://doi.org/10.1016/S1473-3099(04)01046-1 PMID: 15172344
2. Yagupsky P, Dagan R, Prajgrod F, Merires M. Respiratory carriage of *Kingella kingae* among healthy children. The Pediatric Infectious Disease Journal. 1995; 14: 673–678. https://doi.org/10.1097/00006454-199508000-00005 PMID: 8532424
3. Yagupsky P. *Kingella kingae*: Carriage, transmission, and disease. Clinical Microbiology Reviews. 2015. pp. 54–79. https://doi.org/10.1128/CMR.00028-14 PMID: 25567222

4. Gené A, García-García JJ, Sala P, Sierra M, Huguet R. Enhanced culture detection of *Kingella kingae*, a pathogen of increasing clinical importance in pediatrics. Pediatric Infectious Disease Journal. 2004; 23: 886–888. https://doi.org/10.1097/01.INF.0000137591.76624.82 PMID: 15361737

5. Ceroni D, Cherkaoui A, Ferey S, Kaelin A, Schrenzel J. *Kingella kingae* osteoarticular infections in young children: clinical features and contribution of a new specific real-time PCR assay to the diagnosis. Journal of Pediatric Orthopedics. 2010; 30: 301–304. https://doi.org/10.1097/BPO.0b013e3181d4732f PMID: 20357599

6. Chometon S, Benito Y, Chaker M, Boisset S, Ploton C, Bérard J, et al. Specific real-time polymerase chain reaction places *Kingella kingae* as the most common cause of osteoarticular infections in young children. Pediatric Infectious Disease Journal. 2007; 26: 377–381. https://doi.org/10.1097/01.inf.0000259954.88139.f4 PMID: 17468645

7. Kehl-Fie TE, Miller SE, St Geme JW III. *Kingella kingae* expresses type IV pili that mediate adherence to respiratory epithelial and synovial cells. Journal of Bacteriology. 2008; 190: 7157–7163. https://doi.org/10.1128/JB.00884-08 PMID: 18757541

8. Porsch EA, Kehl-Fie TE, St Geme JW III. Modulation of *Kingella kingae* adherence to human epithelial cells by type IV Pili, capsule, and a novel trimeric autotransporter. mBio. 2012; 3: e00372–12. https://doi.org/10.1128/mBio.00372-12 PMID: 23093386

9. Kern BK, Porsch EA, St Geme III JW. Defining the mechanical determinants of *Kingella kingae* adherence to host cells. Journal of Bacteriology. 2017; 199: e00314–17. https://doi.org/10.1128/JB.00314-17 PMID: 28874408

10. Hoppe J, Ünal CM, Thiem S, Grimpe L, Goldmann T, Gaßler N, et al. PilY1 promotes *Legionella pneumophila* infection of human lung tissue explants and contributes to bacterial adhesion, host cell invasion, and twitching motility. Frontiers in Cellular and Infection Microbiology. 2017; 7. https://doi.org/10.3389/fcimb.2017.00063 PMID: 28326293

11. Jonsson AB, Nyberg G, Normark S. Phase variation of gonococcal pili by frameshift mutation in *pilC*, a novel gene for pilus assembly. EMBO Journal. 1991; 10: 477–488. https://doi.org/10.1002/j.1460-2075.1991.tb07970.x PMID: 1671354

12. Rudel T, van Putten JPM, Gibbs CP, Haas R, Meyer TF. Interaction of two variable proteins (PilE and PilC) required for pilus-mediated adherence of *Neisseria gonorrhoeae* to human epithelial cells. Molecular Microbiology. 1992; 6: 3439–3450. https://doi.org/10.1111/j.1365-2958.1992.tb02211.x PMID: 1362447

13. Heiniger RW, Winther-Larsen HC, Pickles RJ, Koomey M, Wolfgang MC. Infection of human mucosal tissue by *Pseudomonas aeruginosa* requires sequential and mutually dependent virulence factors and a novel pilus-associated adhesin. Cellular Microbiology. 2010; 12: 1158–1173. https://doi.org/10.1111/j.1462-5822.2010.01461.x PMID: 20331639

14. Rudel T, Scheuerpflug I, Meyer TF. *Neisseria* PilC protein identified as type-4 pilus tip-located adhesin. Nature. 1995; 373: 357–359. https://doi.org/10.1038/373357a0 PMID: 7830772

15. Morand PC, Tattevin P, Eugene E, Beretti JL, Nassif X. The adhesive property of the type IV pilus-associated component PilC1 of pathogenic *Neisseria* is supported by the conformational structure of the N-terminal part of the molecule. Molecular Microbiology. 2001; 40: 846–856. https://doi.org/10.1046/j.1365-2958.2001.02452.x PMID: 11401692

16. Cheng Y, Johnson MDL, Burillo-Kirch C, Mocny JC, Anderson JE, Garrett CK, et al. Mutation of the conserved calcium-binding motif in *Neisseria gonorrhoeae* PilC1 impacts adhesion but not piliation. Infection and Immunity. 2013; 81: 4279–4289. https://doi.org/10.1128/IAI.00493-13 PMID: 24002068

17. Porsch EA, Johnson MDL, Broadnax AD, Garrett CK, Redinbo MR, St Geme III JW. Calcium binding properties of the *Kingella kingae* PilC1 and PilC2 proteins have differential effects on type IV pilus-mediated adherence and twitching motility. Journal of Bacteriology. 2013; 195: 886–895. https://doi.org/10.1128/JB.02186-12 PMID: 23243304

18. Wolfgang M, Park HS, Hayes SF, van Putten JPM, Koomey M. Suppression of an absolute defect in Type IV pilus biogenesis by loss-of-function mutations in *pilT*, a twitching motility gene in *Neisseria gonorrhoeae*. Proceedings of the National Academy of Sciences of the United States of America. 1998; 95: 14973–14978. https://doi.org/10.1073/pnas.95.25.14973 PMID: 9844000

19. Sambrook J, Fritsch E, Maniatis T. Molecular cloning: a laboratory manual 2nd ed. Cold Spring Harbor, NY: Cold Spring Harbor Laboratory Press; 1989.

20. Prilipov A, Phale P, van Gelder P, Rosenbusch J, Koebnik R. Coupling site-directed mutagenesis with high-level expression: large scale production of mutant porins from *E. coli*. FEMS Microbiology Letters. 1998; 163: 65–72. https://doi.org/10.1111/j.1574-6968.1998.tb13027.x PMID: 9631547

21. Kehl-Fie TE, St Geme III JW. Identification and characterization of an RTX toxin in the emerging pathogen *Kingella kingae*. Journal of Bacteriology. 2007; 189: 430–436. https://doi.org/10.1128/JB.01319-06 PMID: 17098895

22. Hendrixson D, Akerley B, DiRita V. Transposon mutagenesis of *Campylobacter jejuni* identifies a bipartite energy taxis system required for motility. Molecular Microbiology. 2001; 40: 214–224. https://doi.org/10.1046/j.1365-2958.2001.02376.x PMID: 11298288

23. Seifert H. Insertionally inactivated and inducible *recA* alleles for use in *Neisseria*. Gene. 1997; 188: 215–220. https://doi.org/10.1016/s0378-1119(96)00810-4 PMID: 9133594

24. Hamilton H, Schwartz K, Dillard J. Insertion-duplication mutagenesis of *Neisseria*: use in characterization of DNA transfer genes in the gonococcal genetic island. Journal of Bacteriology. 2001; 183: 4718–4726. https://doi.org/10.1128/JB.183.16.4718-4726.2001 PMID: 11466274

25. Guzman L, Belin D, Carson M, Beckwith J. Tight regulation, modulation, and high-level expression by vectors containing the arabinose PBAD promoter. Journal of Bacteriology. 1995; 177: 4121–4130. https://doi.org/10.1128/jb.177.14.4121-4130.1995 PMID: 7608087

26. Orans J, Johnson MDL, Coggan KA, Sperlazza JR, Heiniger RW, Wolfgang MC, et al. Crystal structure analysis reveals *Pseudomonas* PilY1 as an essential calcium-dependent regulator of bacterial surface motility. Proceedings of the National Academy of Sciences of the United States of America. 2010; 107: 1065–1070. https://doi.org/10.1073/pnas.0911616107 PMID: 20080557

27. Kelley LA, Mezulis S, Yates CM, Wass MN, Sternberg MJE. The Phyre2 web portal for protein modeling, prediction and analysis. Nature Protocols. 2015; 10: 845–858. https://doi.org/10.1038/nprot.2015.053 PMID: 25950237

28. Wolfgang M, Lauer P, Park H-SS, Brossay L, Hébert J, Koomey M, et al. PilT mutations lead to simultaneous defects in competence for natural transformation and twitching motility in piliated *Neisseria gonorrhoeae*. Molecular Microbiology. 1998; 29: 321–330. https://doi.org/10.1046/j.1365-2958.1998.00935.x PMID: 9701824

29. Seña AC, Seed P, Nicholson B, Joyce M, Cunningham CK. *Kingella kingae* endocarditis and a cluster investigation among daycare attendees. The Pediatric Infectious Disease Journal. 2010; 29: 86–88. https://doi.org/10.1097/INF.0b013e3181b48cc3 PMID: 19884874

30. Amir J, Yagupsky P. Invasive *Kingella kingae* infection associated with stomatitis in children. The Pediatric Infectious Disease Journal. 1998; 17: 757–758. https://doi.org/10.1097/00006454-199808000-00021 PMID: 9726357

31. Yagupsky P, Press J. Arthritis following stomatitis in a sixteen-month-old child. The Pediatric Infectious Disease Journal. 2003; 22: 573–577. https://doi.org/10.1097/01.inf.0000071414.35517.2c PMID: 12828161

32. Basmaci R, Ilharreborde B, Doit C, Presedo A, Lorrot M, Alison M, et al. Two atypical cases of *Kingella kingae* invasive infection with concomitant human rhinovirus infection. Journal of Clinical Microbiology. 2013; 51: 3137–3139. https://doi.org/10.1128/JCM.01134-13 PMID: 23784119

33. Morand PC, Drab M, Rajalingam K, Nassif X, Meyer TF. *Neisseria meningitidis* Differentially Controls Host Cell Motility through PilC1 and PilC2 Components of Type IV Pili. PLoS ONE. 2009; 4: 6834. https://doi.org/10.1371/journal.pone.0006834 PMID: 19718432

34. Nassif X, Beretti J, Lowy J, Stenberg P, O'Gaora P, Pfeifer J, et al. Roles of pilin and PilC in adhesion of *Neisseria meningitidis* to human epithelial and endothelial cells. Proceedings of the National Academy of Sciences of the United States of America. 1994; 91: 3769–3773. https://doi.org/10.1073/pnas.91.9.3769 PMID: 7909606

35. Johnson MDL, Garrett CK, Bond JE, Coggan KA, Wolfgang MC, Redinbo MR. *Pseudomonas aeruginosa* PilY1 Binds Integrin in an RGD-and Calcium-Dependent Manner. PLoS ONE. 2011; 6: 29629. https://doi.org/10.1371/journal.pone.0029629 PMID: 22242136

36. Scheuerpflug I, Rudel T, Ryll R, Pandit J, Meyer TF. Roles of PilC and PilE Proteins in Pilus-Mediated Adherence of *Neisseria gonorrhoeae* and *Neisseria meningitidis* to Human Erythrocytes and Endothelial and Epithelial Cells. Infection and Immunity. 1999; 67: 834. https://doi.org/10.1128/IAI.67.2.834-843.1999 PMID: 9916098

37. Drake S, Koomey M. The product of the *pilQ* gene is essential for the biogenesis of type IV pili in *Neisseria gonorrhoeae*. Molecular Microbiology. 1995; 18: 975–986. https://doi.org/10.1111/j.1365-2958.1995.18050975.x PMID: 8825101

38. Rudel T, Facius D, Barten R, Scheuerpflug I, Nonnenmacher E, Meyer TF. Role of pili and the phase-variable PilC protein in natural competence for transformation of *Neisseria gonorrhoeae*. Proceedings of the National Academy of Sciences of the United States of America. 1995; 92: 7986–7990. https://doi.org/10.1073/pnas.92.17.7986 PMID: 7644525

39. Berry J-L, Xu Y, Ward PN, Lea SM, Matthews SJ, Pelicic V. A comparative structure/function analysis of two type IV pilin DNA teceptors defines a novel mode of DNA binding. Structure. 2016; 24: 926–934. https://doi.org/10.1016/j.str.2016.04.001 PMID: 27161979

40. Wolfgang M, van Putten JPM, Hayes SF, Koomey M. The *comP* locus of *Neisseria gonorrhoeae* encodes a type IV prepilin that is dispensable for pilus biogenesis but essential for natural

transformation. Molecular Microbiology. 1999; 31: 1345–1357. https://doi.org/10.1046/j.1365-2958.1999.01269.x PMID: 10200956

41. Chen I, Gotschlich EC. ComE, a Competence Protein from *Neisseria gonorrhoeae* with DNA-Binding Activity. Journal of Bacteriology. 2001; 183: 3160–3168. https://doi.org/10.1128/JB.183.10.3160-3168.2001 PMID: 11325945

42. Busch S, Rosenplänter C, Averhoff B. Identification and characterization of *comE* and *comF*, two novel pilin-like competence factors involved in natural transformation of *Acinetobacter* sp. strain BD413. Applied and Environmental Microbiology. 1999; 65: 4568–4574. https://doi.org/10.1128/AEM.65.10.4568-4574.1999 PMID: 10508090

43. Seitz P, Modarres HP, Borgeaud S, Bulushev RD, Steinbock LJ, Radenovic A, et al. ComEA Is Essential for the Transfer of External DNA into the Periplasm in Naturally Transformable *Vibrio cholerae* Cells. PLoS Genetics. 2014; 10: e1004066. https://doi.org/10.1371/journal.pgen.1004066 PMID: 24391524

44. Gangel H, Hepp C, Müller S, Oldewurtel ER, Aas FE, Koomey M, et al. Concerted Spatio-Temporal Dynamics of Imported DNA and ComE DNA Uptake Protein during Gonococcal Transformation. PLoS Pathogens. 2014; 10: e1004043. https://doi.org/10.1371/journal.ppat.1004043 PMID: 24763594

45. Hepp C, Maier B. Kinetics of DNA uptake during transformation provide evidence for a translocation ratchet mechanism. Proceedings of the National Academy of Sciences of the United States of America. 2016; 113: 12472. https://doi.org/10.1073/pnas.1608110113 PMID: 27791096

46. Facius D, Meyer TF. Novel determinant (*comA*) essential for natural transformation competence in *Neisseria gonorrhoeae* and the effect of a *comA* defect on pilin variation. Molecular Microbiology. 1993; 10: 699–712. https://doi.org/10.1111/j.1365-2958.1993.tb00942.x PMID: 7934834

47. Facius D, Fussenegger M, Meyer TF. Sequential action of factors involved in natural competence for transformation of *Neisseria gonorrhoeae*. FEMS Microbiology Letters. 1996; 137: 159–164. https://doi.org/10.1111/j.1574-6968.1996.tb08099.x PMID: 8998979

48. Marathe R, Meel C, Schmidt NC, Dewenter L, Kurre R, Greune L, et al. Bacterial twitching motility is coordinated by a two-dimensional tug-of-war with directional memory. Nature Communications. 2014; 5: 1–10. https://doi.org/10.1038/ncomms4759 PMID: 24806757

49. Merz A, So M, Sheetz M. Pilus retraction powers bacterial twitching motility. Nature. 2000; 407: 98–102. https://doi.org/10.1038/35024105 PMID: 10993081

50. Clausen M, Koomey M, Maier M. Dynamics of type IV pili is controlled by switching between multiple states. Biophysical Journal. 2009; 96: 1169–1177. https://doi.org/10.1016/j.bpj.2008.10.017 PMID: 19186152

51. Zaburdaev V, Biais N, Schmiedeberg M, Eriksson J, Jonsson A-B, Sheetz MP, et al. Uncovering the Mechanism of Trapping and Cell Orientation during *Neisseria gonorrhoeae* Twitching Motility. Biophysical Journal. 2014; 107: 1531. https://doi.org/10.1016/j.bpj.2014.07.061 PMID: 25296304

52. Kehl-Fie TE, Porsch EA, Miller SE, St Geme III JW. Expression of *Kingella kingae* type IV pili is regulated by σ54, PilS, and PilR. Journal of Bacteriology. 2009; 191: 4976–4986. https://doi.org/10.1128/JB.00123-09 PMID: 19465661

53. Starr KF, Porsch EA, Seed PC, Heiss C, Naran R, Forsberg LS, et al. *Kingella kingae* Expresses Four Structurally Distinct Polysaccharide Capsules That Differ in Their Correlation with Invasive Disease. PLoS Pathogens. 2016; 12: e1005944. https://doi.org/10.1371/journal.ppat.1005944 PMID: 27760194

54. Almagro Armenteros JJ, Tsirigos KD, Sønderby CK, Petersen TN, Winther O, Brunak S, et al. SignalP 5.0 improves signal peptide predictions using deep neural networks. Nature Biotechnology. 2019; 37: 420–423. https://doi.org/10.1038/s41587-019-0036-z PMID: 30778233

55. Nielsen H, Engelbrecht J, Brunak S, von Heijne G. Identification of prokaryotic and eukaryotic signal peptides and prediction of their cleavage sites. Protein Engineering, Design and Selection. 1997; 10: 1–6. https://doi.org/10.1093/PROTEIN/10.1.1 PMID: 9051728

56. Micsonai A, Wien F, Kernya L, Lee Y-H, Goto Y, Réfrégiers M, et al. Accurate secondary structure prediction and fold recognition for circular dichroism spectroscopy. Proceedings of the National Academy of Sciences of the United States of America. 2015; 112: E3103. https://doi.org/10.1073/pnas.1500851112 PMID: 26038575

57. Micsonai A, Wien F, Bulyáki É, Kun J, Moussong É, Lee YH, et al. BeStSel: A web server for accurate protein secondary structure prediction and fold recognition from the circular dichroism spectra. Nucleic Acids Research. 2018; 46: W315–W322. https://doi.org/10.1093/nar/gky497 PMID: 29893907

58. Rasband WS. ImageJ. Bethesda, Maryland, USA; 2018. Available: https://imagej.nih.gov/ij/

59. Schneider CA, Rasband WS, Eliceiri KW. NIH Image to ImageJ: 25 years of image analysis. Nature Methods. 2012; 9: 671–675. https://doi.org/10.1038/nmeth.2089 PMID: 22930834